Behavioral/Cognitive

Hippocampal Drift Rate Reflects the Temporal Organization of Memories

Lindsay I. Rait,[1] Guo Wanjia,[1] Zhifang Ye,[1] Sarah DuBrow,[1,2†] and Brice A. Kuhl[1,2]
[1]Department of Psychology, University of Oregon, Eugene, Oregon 97403 and [2]Institute of Neuroscience, University of Oregon, Eugene, Oregon 97403

When freely recalling past events, individuals tend to successively remember stimuli that were studied close together in time—a phenomenon known as temporal clustering. Temporal clustering is thought to occur because stimuli are encoded in relation to a slowly drifting internal context; this internal context representation is then reinstated during recall, leading to clustered recall of stimuli that share a similar internal context. While several lines of evidence implicate the hippocampus in supporting internal context representations, there is limited evidence directly linking hippocampal drift during memory encoding to subsequent temporal clustering during recall. In a human fMRI experiment ($n = 38$; 20 females and 18 males), we sought to influence the rate of internal context change during memory encoding and tested for corresponding effects on (1) temporal clustering and (2) hippocampal drift rate. To influence internal context, we manipulated the rate at which background scenes "switched" while a list of words was encoded. Afterward, subjects freely recalled as many words as possible. While switch rate had no effect on the total number of words recalled, it significantly influenced the degree of temporal clustering. Specifically, a higher switch rate was associated with less temporal clustering. Strikingly, this pattern was mirrored by drift rate in the hippocampus: a higher switch rate was associated with significantly lower hippocampal autocorrelation (more drift). Moreover, individual differences in hippocampal autocorrelation were positively correlated with temporal clustering. Collectively, this suggests that hippocampal drift rate during encoding and temporal clustering during recall each reflects a common internal context representation.

Key words: autocorrelation; episodic memory; fMRI; free recall; hippocampus

Significance Statement

The hippocampus is thought to support a gradually drifting internal context representation that allows memories to be organized in time. This putative internal context representation helps explain the phenomenon of temporal clustering—that events encoded nearby in time are clustered together during recall. Yet, there is surprisingly limited evidence directly linking the drift of hippocampal activity patterns to temporal clustering. Here, we show that manipulating the rate of external context change during memory encoding induced parallel changes in hippocampal drift rate during encoding and temporal clustering during subsequent recall. Critically, hippocampal drift rate also predicted the degree of temporal clustering across individuals. These findings suggest that hippocampal drift rate and temporal clustering reflect a common internal context representation.

Introduction

When freely recalling events from the past, humans tend to spontaneously cluster these events based on the temporal proximity with which they were experienced. In other words, events that are experienced nearby in time tend to be recalled together (Kahana, 1996; Polyn et al., 2009a; Sederberg et al., 2010). This phenomenon—temporal clustering—has been a primary inspiration for an influential class of computation models (temporal context models) which argue that events are encoded in relation to a slowly drifting internal context representation (Howard and Kahana, 2002; Sederberg et al., 2008; Polyn et al., 2009a). The idea behind these models is that if context representations drift slowly, then successive events will be associated with a relatively shared (or stable) context. Later, when one event is recalled from memory, this activates the shared context, thereby cueing recall of other events linked to this context (i.e., temporal

Received May 8, 2025; revised Sept. 6, 2025; accepted Sept. 23, 2025.
Author contributions: L.I.R. and S.D. designed research; L.I.R. performed research; L.I.R., G.W., Z.Y., and B.A.K. analyzed data; L.I.R. and B.A.K. wrote the paper.
We thank J. Benjamin Hutchinson for insightful comments and feedback, and members of the Kuhl lab for helpful discussions. This work was supported by NIH NINDS NS089729 to B.A.K. and by NIH NINDS F31NS126016 to G.W.
This work is dedicated to Sarah DuBrow, who passed away before manuscript completion, but whose impact continues to be felt by many.

†Deceased Feb. 13, 2022.
The authors declare no competing financial interests.
Correspondence should be addressed to Lindsay I. Rait at lrait@uoregon.edu.
https://doi.org/10.1523/JNEUROSCI.0909-25.2025

clustering). While temporal context models have had a major influence on the field of episodic memory, there remains surprisingly limited evidence directly linking temporal clustering in recall to putative neural measures of drifting context representations.

Several lines of evidence support the idea that neural activity patterns drift slowly and that this drift is relevant to episodic memory (MacDonald et al., 2011; DuBrow et al., 2017). For example, when freely recalling a stimulus from memory, electrophysiological measures of neural activity resemble not only the activity pattern that was evoked when that stimulus was originally encoded, but also the activity patterns evoked by stimuli that were encoded nearby in time (Manning et al., 2011). Similarly, successful recognition of a previously encountered stimulus triggers a "jump back" to electrophysiological activity patterns that were temporally adjacent to the original encoding of that stimulus (Howard et al., 2012; Folkerts et al., 2018). The degree of drift in the hippocampus during the encoding of a sequence of stimuli is also predictive of subsequent explicit decisions about the order of, or temporal distance between, those stimuli (Manns et al., 2007; DuBrow and Davachi, 2014; Ezzyat and Davachi, 2014; Jenkins and Ranganath, 2016). Importantly, these distinct lines of evidence have specifically implicated the hippocampus in reflecting drift that is relevant to episodic/temporal memory (Manns et al., 2007; Ezzyat and Davachi, 2014).

Here, we sought to establish a direct link between hippocampal drift rate during encoding and behavioral expressions of spontaneous temporal clustering during subsequent recall. We addressed this in two ways. First, we actively manipulated the rate of external context change during encoding to test whether this had a parallel influence on the rate of hippocampal drift and the degree of subsequent temporal clustering. Motivated by recent fMRI studies (Brunec et al., 2018a; Bouffard et al., 2023), we defined drift rate as the degree of autocorrelation in the fMRI time series, computed at the level of individual voxels. We predicted that higher rates of external context change during encoding (i.e., more event boundaries) would reduce the stability of temporal context representations (DuBrow et al., 2017; Pu et al., 2022), as reflected by a higher hippocampal drift rate (lower autocorrelation) and less temporal clustering during subsequent recall. Second, we tested whether individual differences in hippocampal drift rate during encoding were correlated with the degree of temporal clustering during subsequent recall. We predicted that less drift (higher autocorrelation) would be associated with greater temporal clustering during subsequent recall.

Materials and Methods

Participants

Thirty-nine participants from the University of Oregon and broader community were enrolled in this experiment. One participant was excluded due to technical issues during scanning that prevented completion of the experiment. The final sample size included in analyses was 38 participants (20 female, mean age 21.18 ± 3.85 SD). The sample size was comparable to similar fMRI studies in the field. All participants received monetary compensation for their participation ($25/h). Participants were right-handed, native English speakers, with normal or corrected-to-normal vision, and with no self-reported psychiatric or neurological disorders. Consent was obtained in a manner approved by University of Oregon's Institutional Review Board.

Stimuli

Stimuli consisted of 14 scene images and 192 cue words. Seven scene images depicted an indoor scene and seven depicted an outdoor scene. Scenes were color images taken from the Scene UNderstanding (SUN) database (Xiao et al., 2010). Cue words were two-syllable nouns presented in capitalized letters (e.g., "DAISY") that were based on object image labels from the Bank of Standardized Stimuli (Brodeur et al., 2014). Scene images and cue words were randomly assigned to switch rate conditions uniquely for each participant. All stimuli were presented to participants using PsychoPy (Peirce et al., 2019).

Experimental procedure

The experimental paradigm was modeled after a recent behavioral study (Rait et al., 2024). After providing consent and reviewing the instructions, participants entered the MRI scanner. Participants first completed a brief practice task in the scanner. Then, participants completed the main experimental task, which consisted of eight rounds (each round = 1 scan run). Each round included three sequential phases: encoding, distractor, and immediate recall. Participants then completed a final recall task and two rounds of a visual category localizer task before exiting the scanner. Note: data from the final recall task and the visual category localizer are not described in the current manuscript.

Encoding phase. During the encoding phase, scene images ("contexts") and words were alternately presented (Fig. 1*a*). Specifically, each trial began with the presentation of a scene image (800 pixels by 800 pixels) in the center of the screen (1,000 ms), followed by a fixation cross (500 ms), and then the presentation of a word in the center of the screen (2,500 ms). On each trial, participants were instructed to indicate, using a button box in their right hand, whether or not they would be likely to find the referent of the word within the immediately preceding scene (yes/no). Participants pressed with their index finger to make a "yes" response and with their middle finger to make a "no" response. Participants were instructed to make their response before the word disappeared from the screen. Responses were considered missing if late. After the word, there was a 2,500 ms intertrial interval (ITI) during

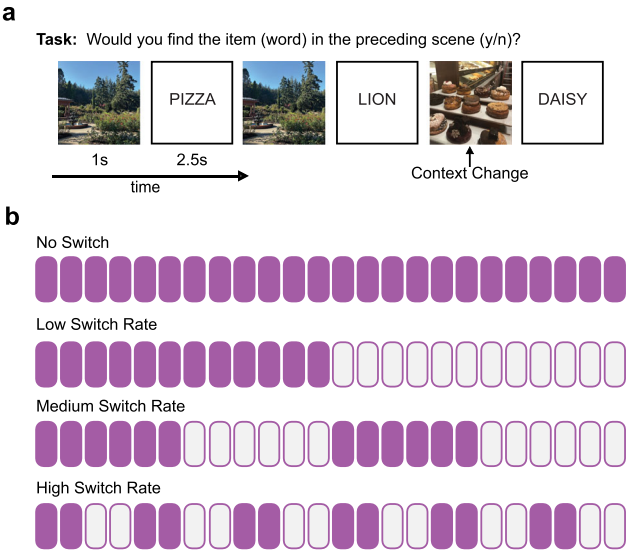

Figure 1. Encoding procedure and design. ***a***, Overview of the encoding task. The encoding phase consisted of alternating presentations of scene and word stimuli. Participants were instructed to respond (yes/no) as to whether or not they would be likely to find each item (word) in the preceding scene. A context change was defined as a change in the scene image. ***b***, Structure of encoding lists. Participants learned eight lists of 24 words each. The rate of context change (context "switch rate") was manipulated across lists, with two lists each for four different switch rate conditions. For the No Switch condition, the context never changed; this condition served as a baseline against which the other conditions were compared. For the Low Switch condition, a single context switch occurred halfway through the list (after 12 items). For the Medium Switch condition, the scene context switched every six items (alternating between two different scenes), resulting in three context switches. For the High Switch condition, the scene context switched after every two items (alternating between two different scenes), resulting in eleven context switches. Context changes are represented by a change in fill color.

which a fixation cross was presented. Each encoding phase included a total of 24 trials. These 24 trials always included 24 unique words and either included one or two different scene images (contexts), depending on the experimental condition (see below, Design). For each word, the immediately preceding scene image was defined as the scene context.

Distractor phase. Following each encoding phase, participants completed a math distractor task consisting of five equations for 15 s in order to reduce rehearsal (Howard and Kahana, 1999). Participants were presented with math equations in the form of $A + B + C = D$, where the values of A, B, and C were set to single digit integers. Participants indicated whether the equation was true or false using a key press (index finger for true, middle finger for false). For false equations, the result (D) differed from the correct sum by either plus or minus one.

Immediate recall phase. After the distractor task, participants saw the word "RECALL" appear on the screen, which indicated the start of the immediate recall phase. During this phase, participants were given 1 min to verbally recall as many words as possible from the encoding phase of the current round. Participants were not given any explicit instructions about the order in which words should be recalled (i.e., it was a free recall task). Responses were recorded via a Persaio microphone in the scanner that was only turned on for recording during the free recall portion of the scan.

Final recall task. After the eight rounds of the main experimental task, participants completed a final recall task during a separate scan run. Participants were given 2 min to verbally recall as many words as they could from the entire experiment, without any explicit instruction about the order in which to recall the words. As in the immediate recall phases, responses were recorded by microphone.

Visual category localizer task. Finally, participants completed a visual category localizer task (two rounds). During this task, all 14 scene images were presented 10 times each (five times per round), in a randomized order. A black fixation cross that was presented in the middle of the scene was red, and participants were instructed to press a button whenever it turned red. Additional details of this task are not included because data from this task are not described in the current manuscript.

Design

For each participant, the eight rounds of the main experimental task included four different "switch rate" conditions (2 rounds each): No Switch, Low, Medium, and High (Fig. 1*b*). These conditions refer to whether the scene context changed within a given encoding phase and, if so, at what rate. For the No Switch condition, the scene context did not change within a given encoding phase (i.e., all 24 words had the same scene context). The No Switch condition was used as a baseline against which the other conditions were compared. For the Low, Medium, and High Switch conditions, each encoding phase included two scene contexts, but the rate of switching between these scene contexts varied. For the Low Switch condition, only a single context switch occurred, halfway through the encoding phase (i.e., after 12 items). For the Medium Switch condition, the scene context switched after every six words; thus, there were three context switches within each Medium Switch encoding phase. For the High Switch condition, the scene context switched after every two words; thus, there were 11 context switches in each High Switch encoding phase. The order of the four switch rate conditions was randomized for each participant with the constraint that each participant had to complete one round of each switch rate condition before a switch rate condition could be repeated. Additionally, each round contained a novel scene (No Switch condition) or pair of scenes (Low, Medium, High Switch conditions) to avoid interference across rounds.

Analysis of behavioral data

Encoding phases. For the encoding phases, we calculated the percentage of trials for which participants responded "yes" versus "no," after removing trials without a response. Mean "yes" versus "no" responses were separately calculated for each switch rate condition.

Immediate recall phases. For the Immediate Recall phases, participants' verbal recall responses were digitally recorded and annotated offline using Penn TotalRecall (http://memory.psych.upenn.edu/TotalRecall). Four undergraduate research assistants, who were blind to which words were randomly assigned to which switch rate condition, transcribed the verbal responses. A recalled word was classified as "valid" if the word was presented during the corresponding encoding phase. Intrusions (i.e., words from previous lists or not in the wordpool) or other vocalizations (e.g., "umm") were excluded from analyses. Additionally, if participants recalled the same word more than once during an immediate recall phase, only the first recall of that word is considered a "valid" recall. We considered three separate measures of memory performance from the immediate recall phases: (1) the total percentage of words recalled, (2) the percentage of boundary and preboundary words recalled, and (3) temporal clustering.

The total percentage of words recalled during each round was defined as the number of "valid" recall words divided by 24 (the total number of words that were encoded).

Recall for boundary and preboundary items was defined as recall for words that immediately followed and immediately preceded a context switch, respectively. The number of boundary/preboundary items differed across the switch rate conditions. In the No Switch condition, because the scene context never switched, there were no boundary or preboundary items. In the Low Switch condition, there was only one boundary item and one preboundary items. For the Medium Switch condition, there were three boundary and three preboundary items. For the High Switch condition, there were 11 boundary and 11 preboundary items. Recall for boundary and preboundary items was therefore expressed as the percentage of these items that were recalled, separately for each of the three conditions in which context switches actually occurred. Note: here we do not consider the first item in a list to be a boundary item.

For each participant, a temporal clustering score was computed separately for each of the eight immediate recall phases, with scores then averaged by switch rate condition (Polyn et al., 2009a). To compute a temporal clustering score for a given study list, we first removed all "invalid" recalls (e.g., intrusions from a prior list) so that only valid recalls remained. For each of these valid recalls (excluding the last recalled word), we then determined the temporal distance during the encoding phase (in absolute positional lag) between that word and the next recalled word (the "actual lag"; Fig. 3*a*), as well as the temporal distances between that word and all other words from the encoding phase that were not yet recalled ("possible lags"). The temporal clustering score was defined as the proportion of possible lags greater than the actual lag. The highest possible temporal clustering score, therefore, would be 1. This would indicate that a participant made the shortest possible recall transitions. A score of 0.5 indicates chance-level temporal clustering, meaning that recall transitions were equally likely to be to a nearby versus remote item. Temporal clustering scores were computed using publicly available MATLAB (The MathWorks) scripts from the Behavioral Toolbox (Version 1.01) from the Computational Memory Lab (http://memory.psych.upenn.edu/Behavioral_toolbox). Temporal clustering scores are initially reported separately for each of the four switch rate conditions. In subsequent analyses, temporal clustering scores are expressed relative to the No Switch condition (i.e., the No Switch condition served as a baseline). Additionally, temporal clustering scores are averaged across the Low and Medium Switch conditions and directly compared with the High Switch condition. The rationale for combining the Low and Medium Switch conditions is that these conditions were relatively similar in terms of total number of context switches per encoding phase (one vs three switches, respectively) and each had many fewer switches than the High Switch condition (11 switches).

For each run, source clustering was calculated by determining the number of recall transitions between items associated with the same scene context and dividing by the total number of recall transitions (Polyn et al., 2009a).

fMRI data acquisition

All scanning was performed on a Siemens 3T Prisma MRI system in the Lewis Center for Neuroimaging at the University of Oregon. Functional images were collected with a T2*-weighted multiband accelerated

echoplanar imaging (EPI) pulse sequence with partial-brain coverage (repetition time, 1,500 ms; echo time, 26 ms; flip angle, 71°; 69 slices, 2 × 2 × 2 mm voxels) and a 64-channel head coil. Note: the total trial length during the encoding phase (6,500 ms) was not a multiple of the repetition time (TR). The use of an "off-TR" design with a relatively short TR was motivated by our focus on autocorrelation in the un-modeled fMRI time series. Additionally, to maximize spatial resolution within the hippocampus and visual cortical regions, we used a high-resolution, partial field-of-view protocol. Slices were oriented parallel to the long-axis of the hippocampus, fully covering the medial temporal lobes and visual cortex, but only partially covering frontal cortex. Each scan for the main experimental task (eight total) consisted of 162 total volumes. The final recall scan (one total) consisted of 88 total volumes. The visual category localizer scans (two total) consisted of 170 total volumes each. All scans included 10 s of lead-in time. Anatomical scans included high-resolution structural T1-weighted whole brain images (3D MPRAGE scan, 1 × 1 × 1 mm voxels) and high-resolution structural T2-weighted coronal images (0.4 × 0.4 × 1.8 mm voxels, perpendicular to the main hippocampus axis) to facilitate segmentation of hippocampal subfields.

Anatomical data preprocessing

fMRI data preprocessing was performed using *fMRIPrep* version 21.0.1 (Esteban et al., 2019), which is based on *Nipype* 1.6.1 (Gorgolewski et al., 2011). The T1-weighted (T1w) image was corrected for intensity non-uniformity (INU) with N4BiasFieldCorrection54 (Tustison et al., 2010) and used as the T1w reference throughout the workflow. The T1w reference was skull-stripped with the antsBrainExtraction.sh workflow (ANTs 2.3.3) in Nipype, using OASIS30ANTs as the target template. Brain tissue segmentation of cerebrospinal fluid (CSF), white matter (WM), and gray matter (GM) was performed on the brain-extracted T1w using fast (FSL 6.0.5.1). Brain surfaces were reconstructed using recon-all from FreeSurfer 6.0.1 (Dale et al., 1999). Volume-based spatial normalization to one standard space (MNI152NLin2009cAsym) was performed through nonlinear registration with antsRegistration (Avants et al., 2008; ANTs 2.3.3), using brain-extracted versions of both T1w reference and the T1w template. *ICBM 152 Nonlinear Asymmetrical template version 2009c* was selected for spatial normalization (Fonov et al., 2009).

Functional data preprocessing

The following preprocessing steps were performed for each of the functional scans for the main experimental rounds (eight total) for each participant using *fMRIPrep*. First, a reference volume and its skull-stripped version were generated by aligning and averaging one single-band reference image (SBRefs). To correct for susceptibility distortions, a field map was estimated based on two (or more) EPI references. The corresponding phase-maps were phase-unwrapped with topup (FSL 6.0.5.1:57b01774). The estimated field maps were then aligned with rigid registration to the target EPI reference run. The field coefficients were mapped onto the reference EPI using the corresponding transform. Functional runs were slice time corrected to half of slice acquisition range using 3dTshift from AFNI (Cox and Hyde, 1997; RRID:SCR_005927). The BOLD reference was then coregistered to the T1w reference using bbregister (FreeSurfer; Greve and Fischl, 2009), resulting in a *preprocessed BOLD* image in T1w space.

After *fMRIPrep* preprocessing, masks generated for each BOLD scan were used to generate one mask based on the intersection of all masks. The first 10 frames (15 s) of each *preprocessed BOLD* were discarded. Additionally, each *processed BOLD* was then scaled at a mean equal 100, with an upper bound of 200 and a lower bound of 0.

Several potentially confounding factors were derived from the *fMRIPrep* output, including six head-motion parameters (three rotations and three translations), framewise displacement (FD), six anatomical CompCor components, and the mean CSF signal. Binary regressors were also created to flag volumes with excessive motion and global signal spikes. Excessive motion volumes were defined as FD > 0.5 mm. Global signal spikes were identified using nltools's find_spikes() function, which flags timepoints with large changes in global signal or its derivative. All 16 of these measures were regressed out from the BOLD time series. For the two binary regressors (excessive motion and global spikes), zeroed-out volumes were replaced by interpolating voxel values from neighboring data points using cubic spline interpolation (Campbell et al., 2013; Brunec et al., 2018a; Thorp et al., 2022). This minimizes any effects of signal spikes while also minimizing potential discontinuities in the fMRI time series. The BOLD time series were resampled into standard space, generating a *preprocessed BOLD* run in MNI152NLin2009cAsym space.

On average, participants had fewer than one interpolated timepoint per run ($M = 0.89$; range, 0–9). Notably, the mean number of interpolated timepoints per participant was not correlated with mean temporal clustering scores (across-subject Spearman correlation: $r_{36} = 0.067$, $p = 0.688$, two-tailed).

Region of interest definition

To generate hippocampal region of interest (ROIs), we used the Automatic Segmentation of Hippocampal Subfields (ASHS; Yushkevich et al., 2015) toolbox with the upenn2017 atlas. This generated subfield ROIs in each participant's hippocampal body: CA3/DG (which included CA3, CA2, and dentate gyrus) and CA1. The most anterior and posterior slices of the hippocampal body were manually determined for each participant based on the T2-weighted anatomical structure (Wanjia et al., 2021). Each participant's subfield segmentations were also manually inspected to ensure the accuracy of the segmentation protocol. Then, each subfield ROI was transformed into each participant's T1-weighted (T1w) space using the T2-to-T1w transformation, calculated with FLIRT (fsl) with six degrees of freedom, implemented with *Nipype*. Following the transformation to T1w space, all ROIs were again visually inspected to ensure that the ROIs were anatomically correct. Whole hippocampal masks were also extracted using FreeSurfer (Fischl, 2012). For each participant, the left and right hippocampal masks were combined and transformed into each participant's T1w space. Hippocampal masks were then split into anterior and posterior segments manually based on the T2-weighted anatomical structure, by using the position of the uncal apex as a conventional anatomical landmark (Poppenk et al., 2013). The anterior (aHPC) and posterior (pHPC) hippocampus ROIs were also visually inspected to ensure the ROIs were anatomically correct.

An ROI for early visual cortex (EVC) was derived from the probabilistic maps of visual topography (Wang et al., 2015) in MNI space, applying a threshold of 0.5. This ROI was then transformed into each participant's native space using inverse T1w-to-MNI nonlinear transformation. Following an approach used by Wanjia et al. (2021), an ROI for the parahippocampal place area (PPA) was created through an automated meta-analysis in Neurosynth using the key term "place." Clusters were then created based on voxels with a *z*-score greater than 2 from the Neurosynth associative tests. Next, we visually inspected the results, given that these clusters were generated through an automated meta-analysis and were not anatomically exclusive to PPA. The two largest clusters that were spatially consistent with PPA were manually selected: one was in the right hemisphere (voxel size = 247) and one in the left hemisphere (voxel size = 163). These clusters were combined into a single PPA mask. This mask was then transformed into each participant's native space using the inverse T1w-to-MNI transformation.

Additional ROIs for exploratory/control analyses were generated for the inferior frontal gyrus (IFG), entorhinal cortex (ERC), angular gyrus, and primary motor cortex (M1). These ROIs were extracted using anatomical labels defined by FreeSurfer's Desikan–Killiany atlas (Desikan et al., 2006). For IFG, the three subregions—pars opercularis, pars orbitalis, and pars triangularis—were combined into a single ROI. Bilateral ERC masks were created by combining left and right entorhinal labels. The same procedure was used to generate bilateral ROIs for the angular gyrus and M1. All ROIs were transformed into each participant's native T1-weighted space and visually inspected to ensure anatomical accuracy.

Autocorrelation analysis

Temporal autocorrelation was computed at the single voxel level (i.e., a separate autocorrelation value for each voxel), following procedures described by Bouffard et al. (2023). For all autocorrelation analyses, we used a lag of 1. Specifically, for each voxel within each ROI, the time series of activity from each encoding phase (i.e., excluding distractor

and immediate recall phases) was temporally shifted by 1 TR (1,500 ms). Then, for each voxel, we calculated the Pearson's correlation between the original time series and the temporally shifted time series.

For analyses that compared autocorrelation across the switch rate conditions, we restricted the autocorrelation measure to timepoints (TRs) that followed the first context switch. Specifically, for the Low, Medium, and High Switch conditions, we selected the first timepoint (TR) that was at least 4 s after the onset of the first context switch (range = 4–5 s after context switch). The exact time windows used for the autocorrelation analyses for each switch rate condition were as follows: Low Switch = 93–166.5 s; Medium Switch = 54–166.5 s; High Switch = 27–166.5 s. Importantly, each of these autocorrelation windows was expressed relative to (or "baselined" against) a corresponding window for the No Switch condition. For example, for the Low Switch condition, autocorrelation was computed for a window from 93 to 166.5 s, and this value was baselined against the exact same time window (93–166.5 s) for the No Switch condition. Thus, the Low, Medium, and High switch conditions each had a unique baseline that was determined by subsampling the No Switch condition. Expressing autocorrelation values relative to a baseline with the same temporal window was intended to correct for any differences in autocorrelation across conditions that might simply be due to differences in the temporal window. Autocorrelation values were Fisher *Z*-transformed and then averaged across voxels and across rounds, producing a single measure of autocorrelation per ROI, subject, and switch rate condition.

Correlation between temporal clustering and hippocampal autocorrelation

Lastly, we correlated temporal clustering scores with autocorrelation values separately for each ROI. In contrast to earlier analyses, autocorrelation was computed across the entire encoding phase—excluding distractor and recall periods—without restricting to timepoints following the first context switch. The rationale for using the entire encoding phase (instead of subsampling) was that temporal clustering scores reflect recall behavior from an entire study list and it is difficult to subsample temporal clustering. Thus, to align temporal clustering with autocorrelation, it makes the most sense to consider the full encoding phase for each measure. Moreover, here we were not interested in differences between conditions but instead in overall differences across participants. Autocorrelations values were Fisher *Z*-transformed, baseline-corrected using the No Switch condition, and averaged to yield one value per ROI, subject, and switch rate condition. Low and Medium Switch conditions were averaged to create a single Low/Medium condition for comparison to the High Switch condition. We ranked temporal clustering scores and autocorrelation values within each condition, averaged the ranks, and computed the Pearson's correlation of these average ranked values. This analysis was motivated by parallel effects of switch rate on both temporal clustering and hippocampal autocorrelation.

Statistical tests

Statistical tests were conducted in R 4.2.3 (R Core Team, 2020). Behavioral and fMRI data were analyzed using a combination of paired *t* tests, repeated-measures ANOVA, generalized linear mixed-effects models, and Pearson's correlations. Effect sizes (i.e., Cohen's *d* and partial eta squared) were calculated using the *lsr* package in R. All *t* tests were two-tailed unless otherwise noted. A threshold of $p < 0.05$ was used to establish statistical significance for all analyses.

Results

Behavioral measures of recall

During the encoding phases, participants indicated whether or not they would be likely to find the referent of each word within the preceding scene context. For trials on which participants made a response, the mean percentage of "yes" responses was 19.77% ± 11.38% (SD). The percentage of "yes" responses did not differ by switch rate condition (No Switch, Low, Medium, High; one-way repeated-measures ANOVA: $F_{(2.77,102.45)} = 0.61$, $p = 0.60$, partial eta squared = 0.02).

During the immediate recall phases, participants attempted to recall as many words as possible from the encoding phase of the current round. The mean percentage of words recalled was 38.51% ± 9.68%. Notably, the mean percentage of words recalled did not differ by switch rate condition (one-way repeated-measures ANOVA: $F_{(2.68,99.29)} = 1.23$, $p = 0.30$, partial eta squared = 0.03; Fig. 2*a*). The lack of an effect of switch rate condition on overall recall is consistent with prior behavioral work (Rait et al., 2024).

We next considered whether recall was influenced by context boundaries (i.e., changes in scene context images). We defined boundary items as words that immediately followed a context change and preboundary items as words that immediately preceded a context change. Thus, because No Switch lists did not include any changes in context, there were no boundary or preboundary items in these lists. A repeated-measures ANOVA with factors of switch rate condition (Low, Medium, High) and boundary status (boundary vs preboundary) revealed a significant main effect of boundary status ($F_{(1,37)} = 8.01$, $p = 0.007$, partial eta squared = 0.18), driven by a higher recall rate for boundary items than preboundary items (Fig. 2*b*). These effects can also be seen in Figure 2*c*, which shows recall probability as a function of serial position, with boundary items highlighted in gray. While the interaction between boundary status and switch rate condition was not significant ($F_{(1.38,51.15)} = 2.99$, $p = 0.077$, partial eta squared = 0.07), post hoc paired-samples *t* tests revealed a significant advantage for boundary items versus preboundary items only for the Low Switch condition (Low: $t_{37} = 2.32$, $p = 0.026$, $d = 0.38$; Medium: $t_{37} = 1.73$, $p = 0.092$, $d = 0.28$; High: $t_{37} = -0.14$, $p = 0.887$, $d = 0.02$).

To better account for the uneven number of event boundaries across the switch rate conditions, we also ran a trial-level mixed-effects model. Specifically, we fit a linear mixed-effects model that predicted trial-level recall accuracy (0 = not recalled, 1 = recalled), with fixed effects for switch rate condition (Low, Medium, High), boundary status (preboundary vs boundary), and their interaction. This model included random intercepts for subject and word identity to account for repeated measures. As in the ANOVA, we observed a significant main effect of boundary status (odds ratio = 2.16, 95% CI = [1.09–4.32], $p = 0.028$), reflecting better recall for boundary items than preboundary items. When specifically considering the High versus Low Switch conditions, there was also a significant interaction between boundary status and switch rate condition (odds ratio = 0.46, 95% CI = [0.22–0.94], $p = 0.033$), reflecting stronger boundary effects for the Low Switch condition compared with the High Switch condition. Thus, recall was enhanced for boundary items, but this effect was most evident when switches occurred less frequently.

Next—and of central interest—we tested whether switch rate condition influenced the degree of temporal clustering of word recall (see Materials and Methods for description of how temporal clustering scores were computed; also see Table 1 for an alternative analysis of clustering by scene category or "source"). A one-way repeated-measures ANOVA with switch rate condition as a factor (No Switch, Low, Medium, High) revealed a significant main effect ($F_{(2.88,106.57)} = 7.83$, $p = 0.0001$, partial eta squared = 0.17) with temporal clustering numerically highest in the Low Switch condition and numerically lowest in the High Switch condition (Fig. 3*b*). Follow-up paired-samples *t* tests revealed that temporal clustering in the Low Switch condition was significantly greater than in the No Switch condition ($t_{(37)} = 2.53$, $p = 0.016$, $d = 0.41$) and High Switch condition

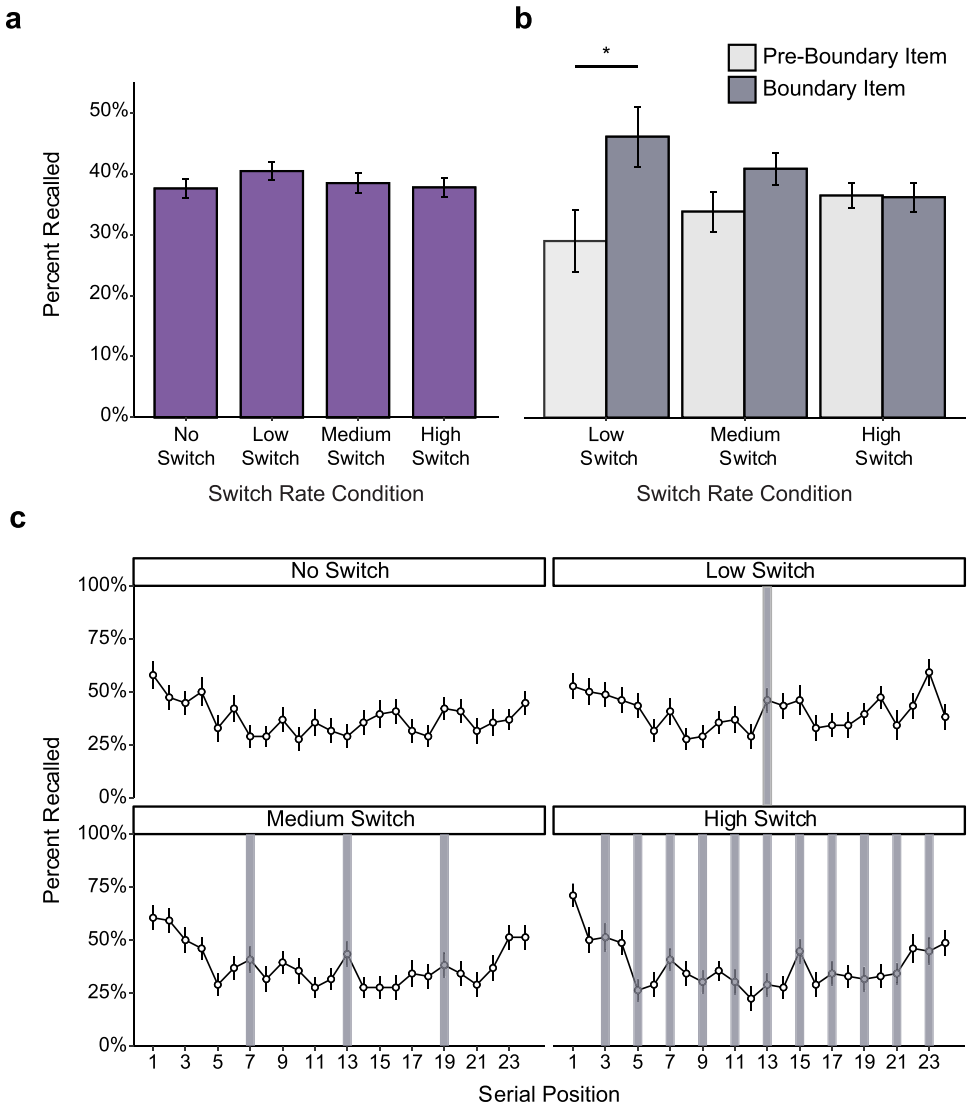

Figure 2. Memory recall by condition and boundaries. ***a***, Percent of words recalled as a function of switch rate condition. There was no difference in the percent of words that participants recalled based on the switch rate condition ($p = 0.30$). ***b***, Percent of words recalled as a function of switch rate condition and boundary status (boundary vs preboundary). Participants recalled more boundary words than preboundary words only in the Low Switch condition ($p = 0.026$). ***c***, Serial position curves for each switch rate condition. Shaded bars reflect boundary items. Note: error bars indicate ±SEM. *$p < 0.05$.

Table 1. Source clustering by switch rate condition

Contrast	Estimate	SE	CI	*p*
Low Switch–Medium Switch	1.50	0.665	0.20–2.80	0.027
Low Switch–High Switch	3.16	0.665	1.86–4.46	<0.001
Medium Switch–High Switch	1.66	0.665	0.34–2.98	0.0148

Source clustering scores (see Materials and Methods) were highest in the Low Switch condition ($M = 0.638 \pm 0.026$), followed by the Medium Switch condition ($M = 0.616 \pm 0.019$) and High Switch condition ($M = 0.512 \pm 0.026$). To test for pairwise differences between switch rate conditions, a linear mixed-effects model was implemented that predicted the number of stay transitions with a fixed effect of switch rate condition and subject as a random intercept. Pairwise comparisons between switch rate conditions are shown in the table.

($t_{(37)} = 4.00$, $p = 0.0003$, $d = 0.65$) but did not differ from the Medium Switch condition ($t_{(37)} = 0.89$, $p = 0.377$, $d = 0.15$). Temporal clustering in the Medium Switch condition was significantly greater than in the High Switch condition ($t_{(37)} = 3.61$, $p = 0.0009$, $d = 0.59$), but did not differ from the No Switch condition ($t_{(37)} = 1.68$, $p = 0.102$, $d = 0.27$). Temporal clustering in the High Switch condition was significantly lower than in the No Switch condition ($t_{(37)} = -2.17$, $p = 0.036$, $d = 0.35$). Thus, while switch rate condition did not influence the overall percentage of studied words that were recalled (Fig. 2*a*), it had a substantial influence on the organization of recall. In particular—and consistent with our prediction—a relatively high context switch rate during encoding disrupted the degree of temporal clustering during recall.

Given the lack of a significant difference in temporal clustering for the Low versus Medium Switch conditions (Fig. 3*b*), for subsequent analyses (temporal clustering and fMRI) we combined (averaged) these two conditions into a single Low/Medium Switch condition. Additionally, in order to better isolate the effects of switch rate, for all subsequent analyses (temporal clustering and fMRI) we used the No Switch condition as a participant-specific baseline that was subtracted from the Low/Medium (before averaging) and High Switch conditions. In other words, Low/Medium and High Switch conditions were expressed relative to the No Switch baseline. Figure 3*c* shows the reformatted data, clearly illustrating that temporal clustering in the Low/Medium Switch condition was higher than baseline, whereas

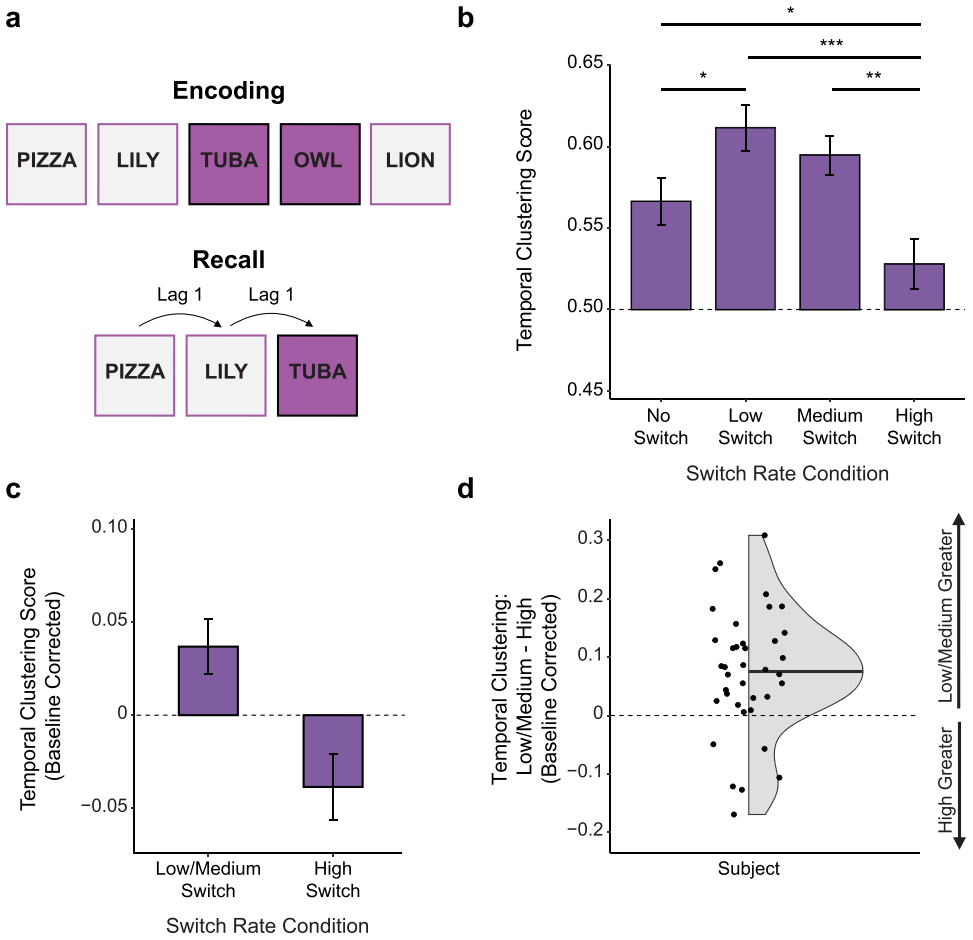

Figure 3. Temporal clustering during memory recall. ***a***, Top, Example subset of an encoding list with context changes reflected by a change in fill color. Bottom, Example subset of a recall list demonstrating high temporal clustering (recall transitions preserve the temporal order from encoding). ***b***, Temporal clustering scores as a function of switch rate condition. Temporal clustering in the High Switch condition was significantly lower than in the No Switch condition ($p = 0.036$), Low Switch condition ($p = 0.0003$), and Medium Switch condition ($p = 0.0009$). There was no difference in temporal clustering scores between the Low and Medium Switch conditions ($p = 0.377$). ***c***, Baseline-corrected temporal clustering scores for the Low/Medium Switch and High Switch conditions (baseline = No Switch condition). ***d***, Baseline-corrected temporal clustering scores for the Low/Medium Switch condition relative to the High Switch condition. Positive scores indicate greater temporal clustering in the Low/Medium Switch condition. Each dot represents an individual participant. Note: error bars indicate ±SEM. *$p < 0.05$, **$p < 0.01$, ***$p < 0.001$.

temporal clustering in the High Switch condition was lower than baseline. The relative increase in temporal clustering in the Low/Medium Switch condition compared with the High Switch condition was evident in most participants (Fig. 3*d*).

fMRI measures of autocorrelation

All fMRI analyses focused on measures of autocorrelation: the degree to which fMRI activation at a given timepoint predicts activation at a subsequent timepoint. Based on leading theories which argue that the hippocampus plays a unique role in tracking context stability (Maurer and Nadel, 2021), we specifically predicted that switch rate condition would influence autocorrelation values in the hippocampus.

To validate our measure of hippocampal autocorrelation, we first sought to replicate a previously reported dissociation in autocorrelation along the long-axis of the hippocampus. Namely, prior studies have shown that autocorrelation values are higher in anterior (aHPC) compared with posterior (pHPC) hippocampus (Brunec et al., 2018a; Bouffard et al., 2023). Averaging data across switch rate conditions, we replicated this finding: autocorrelation values were higher in aHPC compared with pHPC (paired-samples t test: $t_{(37)} = 2.37$, $p = 0.023$, $d = 0.38$; Fig. 4*b*). Given our high-resolution imaging protocol, we also tested for differences between CA1 and CA3/DG—a comparison that, to our knowledge, has not previously been reported. Interestingly, we found higher autocorrelation values in CA3/DG than CA1 ($t_{(37)} = 3.12$, $p = 0.004$, $d = 0.50$; Fig. 4*c*).

Next, we addressed the critical question of whether switch rate condition influenced autocorrelation values in the hippocampus. There were two important features of this analysis: (1) autocorrelation values for each switch rate condition were computed by subsampling the data from each encoding phase to only include timepoints after the first context change (see Materials and Methods) and (2) autocorrelation values for each switch rate condition were baselined against the No Switch condition using a matched subsampling (see Materials and Methods). The rationale for the subsampling (to only include timepoints after the first context change) was that there is no reason why autocorrelation values should differ relative to the No Switch condition before a context change has actually occurred.

Notably, we did not have an a priori prediction that the effect of switch rate condition on autocorrelation would differ across hippocampal subregions. That said, given the overall differences in autocorrelation that we observed in the analyses reported above (Fig. 4), we considered subregions as a factor in our

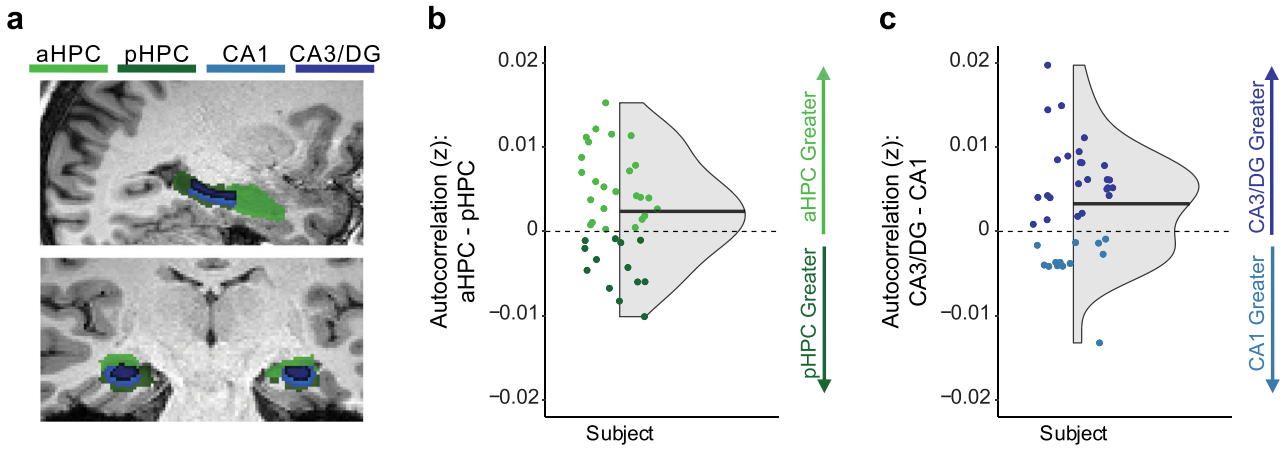

Figure 4. Temporal autocorrelation for hippocampal subregions. ***a***, Hippocampal regions of interest (ROIs) included subregions based on the long-axis of the hippocampus [anterior hippocampus (aHPC), light green; posterior hippocampus (pHPC), dark green], as well as hippocampal subfields [CA1, light blue and CA3, and dentate gyrus (CA3/DG), dark blue]. ***b***, Autocorrelation in aHPC versus pHPC. Autocorrelation was significantly higher in aHPC than pHPC ($p = 0.023$). ***c***, Autocorrelation in CA3/DG versus CA1. Autocorrelation was significantly higher in CA3/DG than CA1 ($p = 0.004$). Notes: data in both graphs are averaged across switch rate conditions; each dot represents an individual participant.

analyses. We first tested for effects across the long-axis of the hippocampus. A two-way repeated-measures ANOVA with factors of ROI (aHPC, pHPC) and switch rate condition (Low/Medium, High) revealed a significant main effect of switch rate ($F_{(1,37)} = 5.25$, $p = 0.028$, partial eta squared = 0.12; Fig. 5*a*), but no main effect of ROI ($F_{(1,37)} = 0.03$, $p = 0.854$, partial eta squared <0.001) and no interaction between switch rate and ROI ($F_{(1,37)} = 0.77$, $p = 0.385$, partial eta squared = 0.02). The main effect of switch rate condition reflected higher autocorrelation in the Low/Medium Switch condition relative to the High Switch condition. In other words, hippocampal activity patterns were relatively more stable when the context was more stable. Note: the lack of a main effect of ROI is not incongruent with the effects shown in Figure 4*b* because, here, autocorrelation values were baselined against the No Switch condition whereas the results in Figure 4*b* are averaged across all switch rate conditions (no baseline correction). Post hoc paired-samples *t* tests indicated that autocorrelation in pHPC was significantly higher in the Low/Medium Switch condition compared with the High Switch condition ($t_{(37)} = 2.46$, $p = 0.018$, $d = 0.40$), with a qualitatively similar pattern in the aHPC ($t_{(37)} = 1.78$, $p = 0.084$, $d = 0.29$).

We next repeated the analysis above, but with CA1 and CA3/DG as the ROIs. Again, the main effect of switch rate condition was significant ($F_{(1,37)} = 5.83$, $p = 0.021$, partial eta squared = 0.14; Fig. 5*b*), with no main effect of ROI ($F_{(1,37)} = 0.78$, $p = 0.384$, partial eta squared = 0.02) or interaction between ROI and switch rate ($F_{(1,37)} = 0.11$, $p = 0.737$, partial eta squared <0.001). Thus, regardless of how we divided the hippocampus, we found that switch rate condition influenced hippocampal autocorrelation. Again, the lack of a main effect of ROI is not incongruent with the effects shown in Figure 4*c* because, here, autocorrelation values were baselined against the No Switch condition whereas the results in Figure 4*c* are averaged across all switch rate conditions (no baseline correction). Post hoc paired-samples *t* tests did not reveal significant differences between the Low/Medium and High Switch conditions for CA1 ($t_{(37)} = 1.80$, $p = 0.080$, $d = 0.29$) or CA3/DG ($t_{(37)} = 2.02$, $p = 0.051$, $d = 0.33$).

To ensure that the autocorrelation results reported above did not reflect any confounding effects of time series interpolation (i.e., interpolation applied to timepoints with excessive motion or global signal spikes; see Materials and Methods), we also implemented separate linear mixed-effects models (one for aHPC and pHPC, and one for CA1 and CA3/DG) that included the number of interpolated timepoints per run as fixed effects. In both cases, the effects of switch rate condition on autocorrelation remained significant (p's < 0.02), confirming that the effects of switch rate condition on autocorrelation were dissociable from any effects of interpolation.

Finally, we tested for effects of switch rate condition (using paired-samples *t* tests) in several regions outside of the hippocampus (Table 2). First, we tested a low-level visual cortical ROI (EVC) and M1, two regions not typically associated with context processing. As expected, there was no effect of switch rate condition (Low/Medium vs High) in EVC ($t_{(37)} = 0.16$, $p = 0.873$, $d = 0.03$) or M1 ($t_{(37)} = 1.27$, $p = 0.207$, $d = 0.21$). Thus, the effects in the hippocampus were not mirroring effects in early visual or motor regions. We next tested a high-level visual cortical ROI sensitive to scene information (PPA). Given that the PPA is specifically sensitive to scene information, we expected it to show an effect of switch rate similar to the hippocampus. Although the effect of switch rate did not reach significance, the pattern of data was qualitatively similar to the posterior hippocampus ($t_{(37)} = 1.98$, $p = 0.055$, $d = 0.32$). Finally, we tested for effects within the angular gyrus, the IFG, and ERC. The rationale for considering the angular gyrus is that it has been implicated in long-timescale integration (Hasson et al., 2015). In contrast, IFG and ERC are regions previously shown to interact with the hippocampus to support temporal memory (DuBrow and Davachi, 2016; Zou et al., 2023). While the angular gyrus and IFG showed no effects of switch rate condition (angular gyrus: $t_{(37)} = 0.41$, $p = 0.682$, $d = 0.07$; IFG: $t_{(37)} = 0.62$, $p = 0.540$, $d = 0.10$), autocorrelation in ERC was significantly higher in the Low/Medium Switch condition compared with the High Switch condition ($t_{(37)} = 2.25$, $p = 0.031$, $d = 0.36$), mirroring effects in the hippocampus. Together, these results highlight that the effect of switch rate on autocorrelation was most evident in the hippocampus and ERC, regions that have each been associated with temporal memory.

Relationship between hippocampal autocorrelation and temporal clustering in recall

Taken together, the behavioral and fMRI results described above indicate that switch rate had parallel effects on temporal clustering and on hippocampal autocorrelation. Specifically, a high

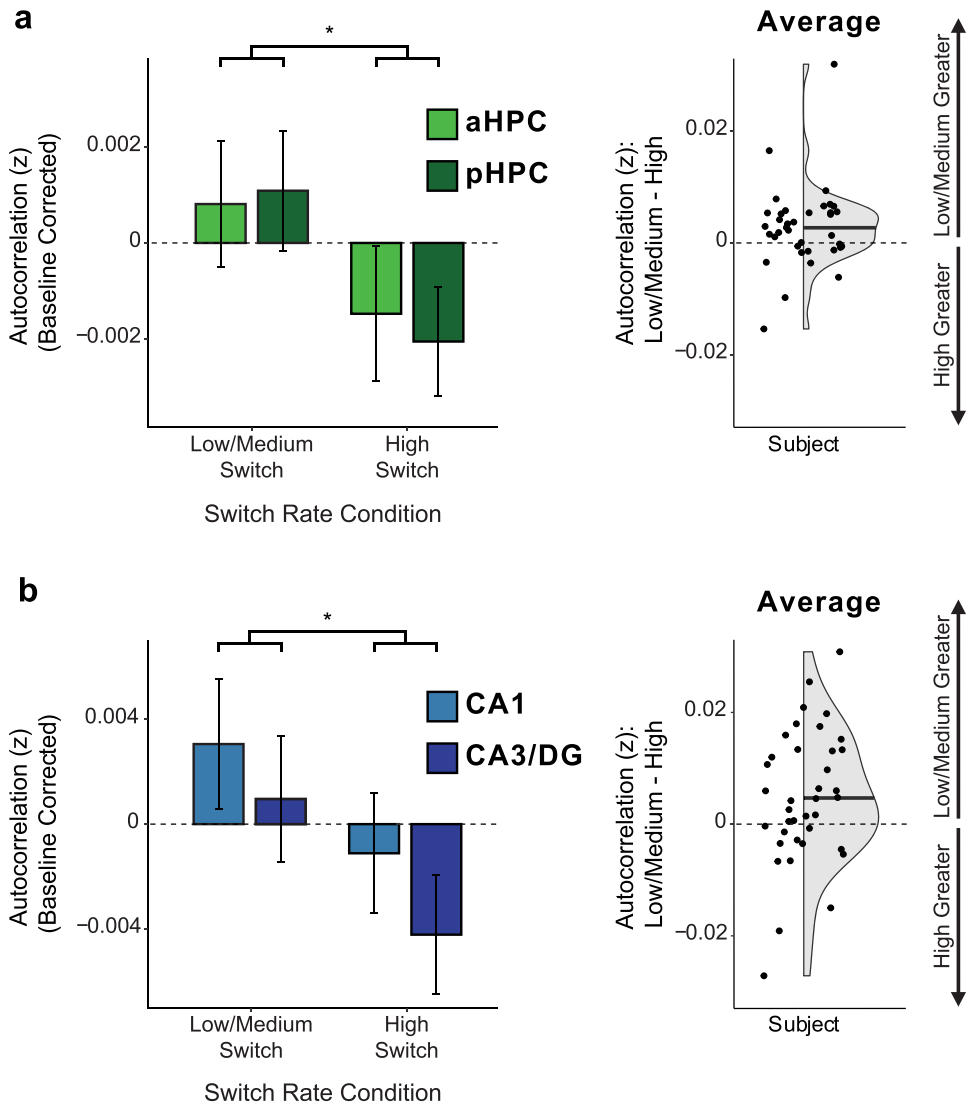

Figure 5. Hippocampal autocorrelation as a function of switch rate condition. ***a***, Left, Autocorrelation in aHPC and pHPC revealed a significant main effect of switch rate condition ($p = 0.028$), reflecting higher autocorrelation in the Low/Medium Switch condition relative to the High Switch condition. Right, Difference between Low/Medium versus High Switch conditions, averaged across aHPC and pHPC; each dot represents an individual participant. ***b***, Autocorrelation CA1 and CA3/DG revealed a main effect of switch rate condition ($p = 0.021$), reflecting higher autocorrelation in the Low/Medium Switch condition relative to the High Switch condition. Right, Difference between Low/Medium versus High Switch conditions, averaged across CA1 and CA3/DG; each dot represents an individual participant. Note: error bars indicate ±SEM. $*p < 0.05$.

Table 2. Autocorrelation effects in nonhippocampal ROIs

	Autocorrelation by switch rate			Brain–behavior correlation	
ROIs	*t* value	*p* value (two-tailed)	Cohen's *d*	*r*	*p* value (one-tailed)
Early visual cortex	0.16	0.873	0.03	0.33	0.020
Parahippocampal place area	1.98	0.055	0.32	0.12	0.241
Primary motor cortex	1.28	0.207	0.21	0.15	0.191
Angular gyrus	0.41	0.682	0.07	0.04	0.403
Inferior frontal gyrus	0.62	0.540	0.10	0.17	0.305
Entorhinal cortex	2.25	0.031	0.36	0.20	0.112

Paired-samples *t* tests compared autocorrelation values for the Low/Medium versus High Switch conditions (positive *t* statistics indicate Low/Medium > High). Of the nonhippocampal ROIs considered, only the entorhinal cortex showed a significant effect of switch rate on autocorrelation ($p = 0.031$). Across-participant correlations tested for relationships between autocorrelation and temporal clustering. Only early visual cortex showed a significant correlation between autocorrelation and temporal clustering.

switch rate was associated with lower temporal clustering of recall and lower autocorrelation in the hippocampus. In a final set of analyses, we tested for a direct relationship between these measures using across-participant correlations. Notably, whereas the autocorrelation analyses reported above subsampled data from each encoding phase to only include timepoints after the first context switch occurred, here no subsampling was applied (see Materials and Methods for rationale). Additionally, in order to obtain a single temporal clustering score per participant and a single autocorrelation score per participant, we averaged data across the Low/Medium and High Switch conditions (see Materials and Methods for details). Importantly, however, the temporal clustering and autocorrelation values were still baselined against the No Switch condition, as in the preceding analyses, to control for global effects. All correlations (Pearson's *r*) were performed on the ranks of temporal clustering and autocorrelation values in order to minimize the influence of extreme values.

Because the preceding analyses indicated that switch rate had similar effects on temporal clustering and hippocampal autocorrelation within participants, we predicted a positive correlation between these variables across participants—i.e., that participants that exhibited higher hippocampal autocorrelation would also exhibit greater temporal clustering. Given this clear a priori prediction, we used one-tailed tests. First, considering ROIs segmented based on the long-axis of the hippocampus, positive correlations between autocorrelation and temporal clustering were observed for aHPC ($r_{(36)} = 0.27$, $p = 0.049$) and pHPC ($r_{(36)} = 0.27$, $p = 0.048$; Fig. 6*a*). Next, considering hippocampal subfields, a positive correlation was observed for CA3/DG ($r_{(36)} = 0.39$, $p = 0.008$) but not CA1 ($r_{(36)} = -0.17$, $p = 0.845$; Fig. 6*b*). There was also a significant difference between the strength of correlations in CA1 versus CA3/DG ($z = 2.43$, $p = 0.015$; two-tailed). These findings establish a direct link between the stability of activity patterns in the hippocampus during encoding and the degree of temporal clustering during subsequent free recall.

Among the nonhippocampal ROIs, only EVC exhibited a correlation between temporal clustering and autocorrelation (Table 2). However, as noted above, EVC did not exhibit within-subject effects of switch rate. Thus, autocorrelation values within the hippocampal ROIs were unique in that they exhibited within-participant effects of switch rate and across-participant relationships with temporal clustering.

Discussion

Here, using a free recall paradigm in which we manipulated the rate of context change during encoding, we establish important links between memory organization (measured by temporal clustering during free recall) and drift rate within the hippocampus (measured by autocorrelation during encoding). While context switch rate had no effect on the total number of words recalled, it powerfully influenced the degree of temporal clustering during subsequent recall. Specifically, a higher context switch rate was associated with relatively less temporal clustering. This result was mirrored by autocorrelation in the hippocampus: a higher context switch rate resulted in relatively lower hippocampal autocorrelation. Finally, we show that participants that exhibited

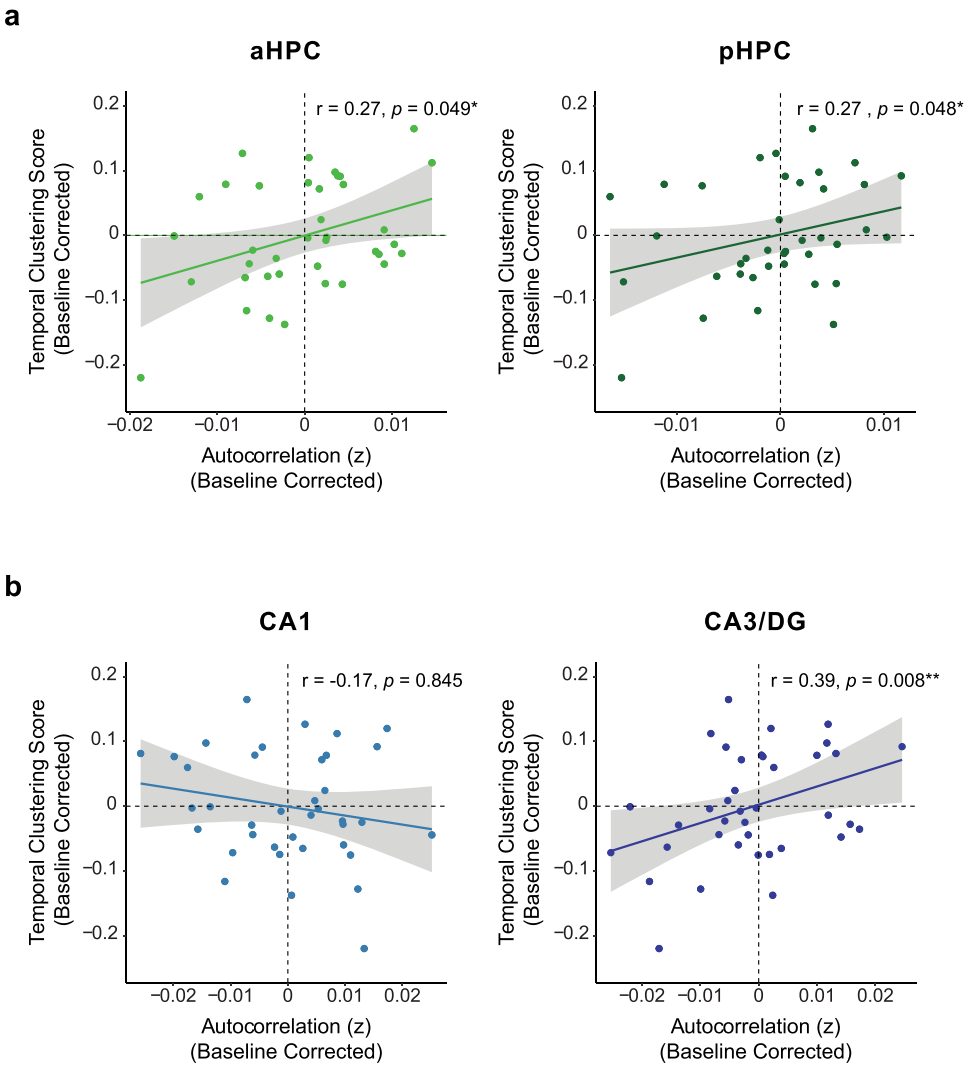

Figure 6. Relationship between hippocampal autocorrelation (during memory encoding) and temporal clustering (during subsequent recall). ***a***, For anterior hippocampus (aHPC; left) and posterior hippocampus (pHPC; right), there were significant, positive correlations (one-tailed) between autocorrelation and temporal clustering (p's < 0.05). ***b***, For CA1, the correlation between autocorrelation and temporal clustering was not significant. For CA3/DG, there was a significant, positive correlation (one-tailed) between autocorrelation and temporal clustering ($p = 0.008$). The correlations in CA1 and CA3/DG were also significantly different from each other ($p = 0.015$). Note: all correlations were performed across participants; each dot represents data from an individual participant. $*p < 0.05$, $**p < 0.01$.

greater hippocampal autocorrelation during encoding also exhibited stronger temporal clustering during free recall.

A key feature of our experimental approach was that we actively manipulated the rate at which the external context (scene images) changed. While the scene images were not explicitly relevant to participants' goals during free recall, our behavioral results clearly demonstrate that changes in external context influenced multiple aspects of recall. First, we found that memory was enhanced (higher recall probability) for items that followed a context shift. This aligns with prior research showing that events that follow an external context change (boundary) are better remembered (Polyn et al., 2009b; Jeunehomme and D'Argembeau, 2020). However, there are also several examples where boundary-related memory enhancement has not been observed (Pettijohn et al., 2016; Gold et al., 2017; Heusser et al., 2018). Here, replicating prior work (Rait et al., 2024), we show that boundary enhancement effects were eliminated when context changes occurred frequently (i.e., in the High Switch condition). Our interpretation of this result is that when context shifts occurred frequently, there was greater "blending" of the context representations (Polyn et al., 2012; Rait et al., 2024) and, correspondingly, context switches were less salient. For example, when switching from Context A (Trials 1 and 2) to Context B (Trials 3 and 4) and then back to A again (Trials 5 and 6), Context A may linger in mind as Trials 3 and 4 are encoded, creating a blended A/B representation. In this case, the "switch" to Context B (Trial 5) should be associated with a weaker prediction error and, correspondingly, a weaker boundary effect (Zacks et al., 2007). If the boundaries themselves are weaker or less salient, then any boundary-related memory enhancement should also be diminished (Clewett et al., 2019). Thus, although the High Switch condition was associated with a higher number of context change events (or because of this), the consequence of individual boundary events was diminished.

Second, and of central interest, we found that switch rate robustly influenced temporal clustering. Our focus on temporal clustering as a behavioral expression of memory organization was motivated by an extensive literature documenting and characterizing temporal clustering effects in free recall (Kahana, 1996; Sederberg et al., 2010; Farrell, 2012). In particular, temporal clustering is thought to be a direct reflection of slowly drifting internal context representations (Howard and Kahana, 2002; Sederberg et al., 2008; Polyn et al., 2009a). While previous research has demonstrated that temporal clustering is a robust phenomenon (Howard and Kahana, 1999, 2002; Healey et al., 2019), our findings add to prior evidence showing that properties of the experimental task or stimuli can have a surprisingly strong impact on the degree of temporal clustering (Manning et al., 2023; Hong et al., 2024). As predicted, we found that the High switch condition was associated with less temporal clustering than the No Switch condition. Interestingly, however, the Low/Medium Switch condition was associated with more temporal clustering than the No Switch condition. Critically, this pattern of results mirrored the effects of switch rate on hippocampal autocorrelation (Fig. 5). We interpret these behavioral and autocorrelation results as reflecting a common influence of external context switch rate on internal context representations. However, this raises the obvious question of: Why would the stability of internal context representations be disrupted by frequent context switches but enhanced by infrequent context switches?

The idea that frequent external context switches disrupt internal context representations is easily reconciled with existing empirical evidence and theoretical arguments related to event boundaries (Polyn et al., 2009a,b; Horner et al., 2016; DuBrow et al., 2017; Brunec et al., 2018b; Clewett et al., 2019; Pu et al., 2022). For example, according to a simple but powerful model (Horner et al., 2016), internal context representations drift slowly in the absence of external context change, but adding an external context change (an event boundary) enhances the drift rate at that boundary (i.e., the change from the preboundary to boundary item). Even though boundaries should only have a temporally localized effect on drift rate (an abrupt shift), they will increase the total drift within a study list (DuBrow et al., 2017). However, this model predicts that infrequent external context switches should have the same effect as frequent switches, just to a lesser degree. In other words, adding event boundaries to a study list should always increase the total drift of internal context representations. That said, accounting for our findings in the Low/Medium Switch condition only requires a minor adjustment to this model. Namely, we can explain the opposing effects of High versus Low/Medium switch conditions simply by assuming that internal context representations are relatively more stable immediately after an event boundary. By this account, event boundaries "reset" the internal context representation (Pu et al., 2022), which not only differentiates the new context from the old context, but temporarily slows the rate of internal context drift. Why might drift rate increase as a function of distance from an event boundary? One possibility is that the external context is most salient immediately after a switch. The temporary salience of a stable external context could translate to a temporary enhancement of the stability of internal context representations. The key feature of this model is that the "cost" of shifting contexts at event boundaries (an abrupt shift in internal context) is offset by an ensuing enhancement in internal context stability. While speculative, this idea provides a simple and intuitive account of our temporal clustering and hippocampal autocorrelation results.

By showing that hippocampal drift rate parallels (Fig. 5) and predicts (Fig. 6) differences in temporal clustering, our findings add to a substantial literature implicating the hippocampus in the temporal organization of memory (Eichenbaum, 2014; Davachi and DuBrow, 2015; Long and Kahana, 2015; Goyal et al., 2018; Yoo et al., 2021; Zheng et al., 2022; Zou et al., 2023). More specifically, our findings complement a growing body of evidence—across multiple different paradigms and experimental approaches—demonstrating the relevance of drift within the hippocampus (or medial temporal lobes, more generally) to subsequent expressions of temporal memory (Manns et al., 2007; Manning et al., 2011; DuBrow and Davachi, 2014; Ezzyat and Davachi, 2014; Jenkins and Ranganath, 2016; Folkerts et al., 2018; El-Kalliny et al., 2019; Umbach et al., 2020). Our findings are also relevant to prior evidence for functional specialization along the long axis of the hippocampus, both in humans (Poppenk et al., 2013; Brunec et al., 2018a; Thorp et al., 2022; Bouffard et al., 2023) and rodents (Moser and Moser, 1998; Fanselow and Dong, 2010; Komorowski et al., 2013). For example, prior research in humans has shown that the anterior hippocampus (aHPC) maintains coarser-grained representations, characterized by more stable and slowly drifting signals over time, compared with the posterior hippocampus (pHPC; Brunec et al., 2018a; Bouffard et al., 2023). We replicate this anterior-to-posterior gradient (Fig. 4*b*) in hippocampal autocorrelation but also demonstrate a novel distinction across hippocampal subfields. Specifically, we found higher autocorrelation (more stability) in CA3/DG than CA1 (Fig. 4*c*). Interestingly, however, the effects of switch rate did not statistically differ

across aHPC versus pHPC or across CA3/DG versus CA1. Thus, while overall drift rate varied across subregions of the hippocampus, sensitivity to external context shifts was relatively uniform. That said, the across-participant relationship between autocorrelation and temporal clustering was stronger in CA3/DG than in CA1. Given that this is not a dissociation we predicted in advance—or one with an obvious precedent in the literature—it will be of interest in future research to further characterize potential differences in the behavioral relevance of drift rate with CA3/DG versus CA1. Additionally, it will be valuable in future research to establish within-participant relationships between autocorrelation and temporal clustering (in contrast to the across-participant relationships reported here).

In conclusion, our findings provide important evidence that drift rate within the hippocampus is linked to the rate of external context change and to the temporal organization of free recall. These findings support and extend influential computational models which describe how context shapes memory (Howard and Kahana, 2002; Sederberg et al., 2008; Polyn et al., 2009a).

References

Avants BB, Epstein CL, Grossman M, Gee JC (2008) Symmetric diffeomorphic image registration with cross-correlation: evaluating automated labeling of elderly and neurodegenerative brain. Med Image Anal 12:26–41.

Bouffard NR, Golestani A, Brunec IK, Bellana B, Park JY, Barense MD, Moscovitch M (2023) Single voxel autocorrelation uncovers gradients of temporal dynamics in the hippocampus and entorhinal cortex during rest and navigation. Cereb Cortex 33:3265–3283.

Brodeur MB, Guérard K, Bouras M (2014) Bank of standardized stimuli (BOSS) phase II: 930 new normative photos. PLoS One 9:e106953.

Brunec IK, et al. (2018a) Multiple scales of representation along the hippocampal anteroposterior axis in humans. Curr Biol 28:2129–2135.e6.

Brunec IK, Moscovitch M, Barense MD (2018b) Boundaries shape cognitive representations of spaces and events. Trends Cogn Sci 22:637–650.

Campbell K, Grigg O, Saverino C, Churchill N, Grady C (2013) Age differences in the intrinsic functional connectivity of default network subsystems. Front Aging Neurosci 5:73.

Clewett D, DuBrow S, Davachi L (2019) Transcending time in the brain: how event memories are constructed from experience. Hippocampus 29:162–183.

Cox RW, Hyde JS (1997) Software tools for analysis and visualization of fMRI data. NMR Biomed 10:171–178.

Dale AM, Fischl B, Sereno MI (1999) Cortical surface-based analysis: I. segmentation and surface reconstruction. Neuroimage 9:179–194.

Davachi L, DuBrow S (2015) How the hippocampus preserves order: the role of prediction and context. Trends Cogn Sci 19:92–99.

Desikan RS, et al. (2006) An automated labeling system for subdividing the human cerebral cortex on MRI scans into gyral based regions of interest. Neuroimage 31:968–980.

DuBrow S, Rouhani N, Niv Y, Norman KA (2017) Does mental context drift or shift? Curr Opin Behav Sci 17:141–146.

DuBrow S, Davachi L (2014) Temporal memory is shaped by encoding stability and intervening item reactivation. J Neurosci 34:13998–14005.

DuBrow S, Davachi L (2016) Temporal binding within and across events. Neurobiol Learn Mem 134:107–114.

Eichenbaum H (2014) Time cells in the hippocampus: a new dimension for mapping memories. Nat Rev Neurosci 15:732–744.

El-Kalliny MM, Wittig JH, Sheehan TC, Sreekumar V, Inati SK, Zaghloul KA (2019) Changing temporal context in human temporal lobe promotes memory of distinct episodes. Nat Commun 10:203.

Esteban O, et al. (2019) fMRIPrep: a robust preprocessing pipeline for functional MRI. Nat Methods 16:111–116.

Ezzyat Y, Davachi L (2014) Similarity breeds proximity: pattern similarity within and across contexts is related to later mnemonic judgments of temporal proximity—ScienceDirect. https://www.sciencedirect.com/science/article/pii/S0896627314000737

Fanselow MS, Dong H-W (2010) Are the dorsal and ventral hippocampus functionally distinct structures? Neuron 65:7–19.

Farrell S (2012) Temporal clustering and sequencing in short-term memory and episodic memory. Psychol Rev 119:223–271.

Fischl B (2012) Freesurfer. Neuroimage 62:774–781.

Folkerts S, Rutishauser U, Howard MW (2018) Human episodic memory retrieval is accompanied by a neural contiguity effect. J Neurosci 38:4200–4211.

Fonov V, Evans A, McKinstry R, Almli C, Collins D (2009) Unbiased nonlinear average age-appropriate brain templates from birth to adulthood. Neuroimage 47:S102.

Gold DA, Zacks JM, Flores S (2017) Effects of cues to event segmentation on subsequent memory. Cogn Res Princ Implic 2:1.

Gorgolewski K, Burns CD, Madison C, Clark D, Halchenko YO, Waskom ML, Ghosh SS (2011) Nipype: a flexible, lightweight and extensible neuroimaging data processing framework in python. Front Neuroinform 5:13.

Goyal A, et al. (2018) Electrical stimulation in hippocampus and entorhinal cortex impairs spatial and temporal memory. J Neurosci 38:4471–4481.

Greve DN, Fischl B (2009) Accurate and robust brain image alignment using boundary-based registration. Neuroimage 48:63–72.

Hasson U, Chen J, Honey CJ (2015) Hierarchical process memory: memory as an integral component of information processing. Trends Cogn Sci 19:304–313.

Healey MK, Long NM, Kahana MJ (2019) Contiguity in episodic memory. Psychon Bull Rev 26:699–720.

Heusser AC, Ezzyat Y, Shiff I, Davachi L (2018) Perceptual boundaries cause mnemonic trade-offs between local boundary processing and across-trial associative binding. J Exp Psychol Learn Mem Cog 44:1075–1090.

Hong MK, Gunn JB, Fazio LK, Polyn SM (2024) The modulation and elimination of temporal organization in free recall. J Exp Psychol Learn Mem Cogn 50:1035–1068.

Horner AJ, Bisby JA, Wang A, Bogus K, Burgess N (2016) The role of spatial boundaries in shaping long-term event representations. Cognition 154:151–164.

Howard MW, Viskontas IV, Shankar KH, Fried I (2012) Ensembles of human MTL neurons "jump back in time" in response to a repeated stimulus. Hippocampus 22:1833–1847.

Howard MW, Kahana MJ (1999) Contextual variability and serial position effects in free recall. J Exp Psychol Learn Mem Cogn 25:923–941.

Howard MW, Kahana MJ (2002) A distributed representation of temporal context. J Math Psychol 46:269–299.

Jenkins LJ, Ranganath C (2016) Distinct neural mechanisms for remembering when an event occurred. Hippocampus 26:554–559.

Jeunehomme O, D'Argembeau A (2020) Event segmentation and the temporal compression of experience in episodic memory. Psychol Res 84:481–490.

Kahana MJ (1996) Associative retrieval processes in free recall. Mem Cognit 24:103–109.

Komorowski RW, Garcia CG, Wilson A, Hattori S, Howard MW, Eichenbaum H (2013) Ventral hippocampal neurons are shaped by experience to represent behaviorally relevant contexts. J Neurosci 33:8079–8087.

Long NM, Kahana MJ (2015) Successful memory formation is driven by contextual encoding in the core memory network. Neuroimage 119:332–337.

MacDonald CJ, Lepage KQ, Eden UT, Eichenbaum H (2011) Hippocampal "time cells" bridge the gap in memory for discontiguous events. Neuron 71:737–749.

Manning JR, Polyn SM, Baltuch GH, Litt B, Kahana MJ (2011) Oscillatory patterns in temporal lobe reveal context reinstatement during memory search. Proc Natl Acad Sci U S A 108:12893–12897.

Manning JR, Whitaker EC, Fitzpatrick PC, Lee MR, Frantz AM, Bollinger BJ, Romanova D, Field CE, Heusser AC (2023) Feature and order manipulations in a free recall task affect memory for current and future lists. *arXivorg*. https://par.nsf.gov/biblio/10394641-feature-order-manipulations-free-recall-task-affect-memory-current-future-lists

Manns JR, Howard MW, Eichenbaum H (2007) Gradual changes in hippocampal activity support remembering the order of events. Neuron 56:530–540.

Maurer AP, Nadel L (2021) The continuity of context: a role for the hippocampus. Trends Cogn Sci 25:187–199.

Moser M-B, Moser EI (1998) Functional differentiation in the hippocampus. Hippocampus 8:608–619.

Peirce J, Gray JR, Simpson S, MacAskill M, Höchenberger R, Sogo H, Kastman E, Lindeløv JK (2019) Psychopy2: experiments in behavior made easy. Behav Res Methods 51:195–203.

Pettijohn KA, Thompson AN, Tamplin AK, Krawietz SA, Radvansky GA (2016) Event boundaries and memory improvement. Cognition 148:136–144.
Polyn SM, Norman KA, Kahana MJ (2009a) A context maintenance and retrieval model of organizational processes in free recall. Psychol Rev 116:129–156.
Polyn SM, Norman KA, Kahana MJ (2009b) Task context and organization in free recall. Neuropsychologia 47:2158–2163.
Polyn SM, Kragel JE, Morton NW, McCluey JD, Cohen ZD (2012) The neural dynamics of task context in free recall. Neuropsychologia 50:447–457.
Poppenk J, Evensmoen HR, Moscovitch M, Nadel L (2013) Long-axis specialization of the human hippocampus. Trends Cogn Sci 17:230–240.
Pu Y, Kong X-Z, Ranganath C, Melloni L (2022) Event boundaries shape temporal organization of memory by resetting temporal context. Nat Commun 13:622.
Rait LI, Murty VP, DuBrow S (2024) Contextual familiarity rescues the cost of switching. Psychon Bull Rev 31:1103–1113.
R Core Team (2020) R: A language and environment for statistical computing. R Foundation for Statistical Computing, Vienna, Austria. https://www.R-project.org/
Sederberg PB, Howard MW, Kahana MJ (2008) A context-based theory of recency and contiguity in free recall. Psychol Rev 115:893.
Sederberg PB, Miller JF, Howard MW, Kahana MJ (2010) The temporal contiguity effect predicts episodic memory performance. Mem Cognit 38: 689–699.
Thorp JN, Gasser C, Blessing E, Davachi L (2022) Data-driven clustering of functional signals reveals gradients in processing both within the anterior hippocampus and across its long axis. J Neurosci 42:7431–7441.
Tustison NJ, Avants BB, Cook PA, Zheng Y, Egan A, Yushkevich PA, Gee JC (2010) N4ITK: improved N3 bias correction. IEEE Trans Med Imaging 29:1310–1320.
Umbach G, Kantak P, Jacobs J, Kahana M, Pfeiffer BE, Sperling M, Lega B (2020) Time cells in the human hippocampus and entorhinal cortex support episodic memory. Proc Natl Acad Sci U S A 117:28463–28474.
Wang L, Mruczek REB, Arcaro MJ, Kastner S (2015) Probabilistic maps of visual topography in human cortex. Cereb Cortex 25:3911–3931.
Wanjia G, Favila SE, Kim G, Molitor RJ, Kuhl BA (2021) Abrupt hippocampal remapping signals resolution of memory interference. Nat Commun 12: 4816.
Xiao J, Hays J, Ehinger KA, Oliva A, Torralba A (2010) SUN database: large-scale scene recognition from abbey to zoo. 2010 IEEE Computer Society Conference on Computer Vision and Pattern Recognition, 3485–3492.
Yoo HB, Umbach G, Lega B (2021) Neurons in the human medial temporal lobe track multiple temporal contexts during episodic memory processing. Neuroimage 245:118689.
Yushkevich PA, Pluta JB, Wang H, Xie L, Ding S-L, Gertje EC, Mancuso L, Kliot D, Das SR, Wolk DA (2015) Automated volumetry and regional thickness analysis of hippocampal subfields and medial temporal cortical structures in mild cognitive impairment. Hum Brain Mapp 36:258–287.
Zacks JM, Speer NK, Swallow KM, Braver TS, Reynolds JR (2007) Event perception: a mind/brain perspective. Psychol Bull 133:273–293.
Zheng J, Schjetnan AGP, Yebra M, Gomes BA, Mosher CP, Kalia SK, Valiante TA, Mamelak AN, Kreiman G, Rutishauser U (2022) Neurons detect cognitive boundaries to structure episodic memories in humans. Nat Neurosci 25:358–368.
Zou F, Wanjia G, Allen EJ, Wu Y, Charest I, Naselaris T, Kay K, Kuhl BA, Hutchinson JB, DuBrow S (2023) Re-expression of CA1 and entorhinal activity patterns preserves temporal context memory at long timescales. Nat Commun 14:4350.